01 May 2009

Novel Near-Field Millimeter-Wave Differential Probe using a Loaded Modulated Aperture

Mohamed A. Abou-Khousa

Sergey Kharkovsky
Missouri University of Science and Technology

R. Zoughi
Missouri University of Science and Technology, zoughi@mst.edu

Recommended Citation

M. A. Abou-Khousa et al., "Novel Near-Field Millimeter-Wave Differential Probe using a Loaded Modulated Aperture," *IEEE Transactions on Instrumentation and Measurement*, vol. 58, no. 5, pp. 1273-1282, Institute of Electrical and Electronics Engineers (IEEE), May 2009.
The definitive version is available at https://doi.org/10.1109/TIM.2008.2009131

Novel Near-Field Millimeter-Wave Differential Probe Using a Loaded Modulated Aperture

Mohamed A. Abou-Khousa, *Student Member, IEEE*, Sergey Kharkovsky, *Senior Member, IEEE*, and Reza Zoughi, *Fellow, IEEE*

***Abstract*—Near-field millimeter-wave techniques have effectively been used for nondestructive testing (NDT) and imaging applications for over a decade. The interaction of the fields and a structure under test (SUT) in the near field of a probe is more complex than that of the far-field interaction. In the near field, the distance between the probe and the SUT, which is referred to as the standoff distance, is an important measurement parameter, and when optimally chosen, it can significantly improve detection sensitivity. However, undesired changes in this parameter can adversely influence the detection outcome to the extent that a target may be totally masked. Consequently, in the past, several different methods and remedies have been proposed to eliminate or drastically reduce this adverse influence, each with its own limitations. In this paper, a novel method involving a probing waveguide aperture loaded with two small modulated antennas is introduced, which operates in a differential mode and is capable of automatically eliminating undesired changes in the standoff distance during testing. In addition, this differential probe efficiently overcomes the limitations of the previously developed methods. The proposed probe is based on electronic modulation of the dominant aperture field of the rectangular waveguide using p-i-n diode-loaded dipoles symmetrically placed in the aperture. This paper presents the design of this unique probe, and the results show that the adverse effect of the standoff distance variation can be eliminated or otherwise significantly reduced by noncoherently subtracting the signals measured at two different aperture modulation states.**

***Index Terms*—Differential probes, loaded dipoles, microwave and millimeter-wave nondestructive testing (NDT), modulated apertures, near-field imaging, p-i-n diode, standoff distance variations.**

I. Introduction

NEAR-FIELD microwave and millimeter-wave nondestructive testing (NDT) and imaging techniques have shown great utility for a wide range of applications. Reflectometer probes with open-ended rectangular waveguide apertures as probing antennas are commonly used for near-field NDT and imaging. The open-ended waveguide aperture is used to illuminate the structure under test (SUT) and to receive the reflected signal. The detection system is designed to produce a dc signal proportional to the phase and/or magnitude of the reflected signal. In most cases, the detection system may simply consist of a diode detector (e.g., a standing-wave reflectometer). For imaging purposes, the waveguide aperture is scanned over the SUT, and the measured output dc signal is mapped into a 2-D intensity raster image [1].

Near-field probes are intrinsically sensitive to variations in the distance between the probing antenna and the structure under inspection, i.e., the standoff distance [1]. Such variations can potentially mask the signal of interest in an image, such as the signal due to a defect or an anomaly and, hence, adversely influence the detection capability of the probe. Consequently, it is imperative that the standoff distance is kept constant during the scanning process. While this is somewhat manageable for structures with relatively flat surfaces, it is rather difficult to be achieved for curved surfaces or when the standoff distance changes as a result of vibrations frequently encountered in practice (i.e., imaging a conveyed material). Moreover, a change in the standoff distance becomes more of a problem at high frequencies, at which finer spatial resolutions are possible for detecting small defects, and the field properties more significantly change as a function of and in the direction of propagation [1], [2].

Several solutions have been proposed in the past to eliminate or compensate for the adverse effect of the standoff distance variation. These solutions can be divided into two categories, namely, noncoherent and coherent methods. Noncoherent standoff distance compensation methods involve the concurrent detection and processing of two signals noncoherently (i.e., without considering phase information). While one of the detected signals solely maps the standoff distance variation, the second signal bears the information due to the standoff distance variation and the signal of interest. Thus, by special processing, the signal due only to the standoff distance variation can be used to eliminate this influence from the second signal. The methods proposed in [3] and [4] belong to this category. These methods, although modest in complexity, require special scaling, i.e., calibration, and typically offer a relatively small range of standoff distance compensation, e.g., less than a quarter of the wavelength. The simplicity of these methods stems from the fact that they are based on noncoherent detection.

On the other hand, coherent compensation is based on coherently subtracting two signals using their phases and magnitudes. As in the noncoherent methods, one of the processed signals carries the standoff distance information, and the second contains both the signal of interest and the signal due to the standoff distance. To realize both signals simultaneously, two spatially spaced waveguide apertures are incorporated when

Manuscript received June 25, 2008; revised October 6, 2008. First published January 6, 2009; current version published April 7, 2009. The Associate Editor coordinating the review process for this paper was Dr. Yves Rolain.

The authors are with the Applied Microwave Nondestructive Testing Laboratory, Department of Electrical and Computer Engineering, Missouri University of Science and Technology, Rolla, MO 65409 USA (e-mail: maamc2@mst.edu; sergiy@mst.edu; zoughir@mst.edu).

Color versions of one or more of the figures in this paper are available online at http://ieeexplore.ieee.org.

Digital Object Identifier 10.1109/TIM.2008.2009131

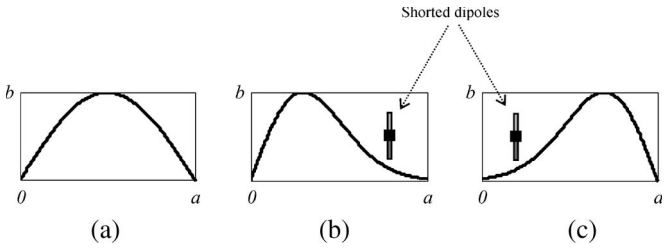

Fig. 1. Aperture relative electric field magnitude distribution for the (a) TE_{10} mode of an unloaded waveguide aperture, (b) loaded aperture with a shorted dipole placed toward the right aperture side, and (c) loaded aperture with a shorted dipole placed toward the left aperture side.

scanning the structure [5]. The probe proposed in [5] is based on two radiating apertures whereby a magic-T is used to coherently subtract the signals reflected from both apertures. This method offers a standoff distance compensation range beyond one wavelength, which is a significant distance. While such a differential probe is highly effective, its design is more complex compared to the noncoherent methods.

However, a noncoherent (simple) differential probe that can offer a large compensation range compared to the previously proposed methods has not yet been developed. To this end, a near-field microwave and millimeter-wave differential probe based on a novel dual-loaded modulated single waveguide aperture has recently been designed and developed [6]. Using this novel design, the undesired influence of the standoff distance variation can be eliminated or otherwise significantly reduced by noncoherently detecting and subtracting the signals measured at two different aperture modulation states. In this paper, we present a detailed analysis of the dual-loaded modulated aperture probe and extend the results beyond the preliminary experimental investigation reported in [6]. In particular, we validate the probe concept and investigate its response, sensitivity, and resolution via numerical electromagnetic simulations. Such analysis provides insight into the probe design and helps in better understanding of the probe capability in near-field millimeter-wave imaging applications.

II. Dual-Loaded Aperture Probe Concept

The proposed probe is based on switching between two electric field distributions synthesized over a single rectangular waveguide aperture of dimensions $a \times b$. To illustrate this idea, consider Fig. 1(a) showing the relative magnitude distribution of the aperture electric field when the dominant mode TE_{10} is incident on the aperture [2]. When a small short-circuited dipole is placed close to the aperture sidewall, as shown in Fig. 1(b), the electric field distribution becomes skewed with its peak shifted in the opposite direction away from the shorted dipole. A mirror distribution is obtained if the shorted dipole is placed at the other side of the aperture, as shown in Fig. 1(c).

It is important to note that the aperture fields shown in Fig. 1 are for illustration purposes only since placing a dipole inside the aperture region not only changes the dominant mode distribution [as depicted in Fig. 1(b) and (c)] but might also cause higher order modes to be generated. The actual field distribution in the loaded aperture region will be obtained and shown later using full-wave numerical simulations.

In light of the aforementioned discussion, when two identical center-loaded dipoles are symmetrically placed inside the aperture region, two "mirror" electric field distributions can be synthesized by electronically controlling the loads of the dipoles. The dipoles, each of length l, are separated by a distance s along the broad aperture dimension a, as shown in Fig. 2(a). To explain the idea, assume that the loads of the dipoles can electronically be set to an open or a short. The effect of these loads can approximately be realized in practice using p-i-n diodes to load the dipoles and turning them "OFF" and "ON," respectively [7], [8], as used in the prototype probe that will be described later.

When one of dipoles is open-circuited and the other is short-circuited, the distribution is skewed toward the open-circuited dipole. The skew direction is reversed by reversing the dipole loading states. Both of the mirror distributions interact with their surroundings in a similar manner, and by switching between them during the scanning, i.e., turning one of them "ON" at a time through modulation, two signals can be measured at any scan location. Effectively in this case, both aperture distributions are used to scan the SUT. Now, if the standoff distance varies along the narrow dimension of the waveguide aperture b, the effect of this variation on the measured signal is independent of which distribution is turned "ON." This entails that the effect of the standoff distance on the signal measured while one of the distributions is turned "ON" is identical to its effect on the signal measured while the mirror distribution is turned "ON." Consequently, the undesired standoff variation effect can be compensated by subtracting the measured signals. It is also important to note that the scanning speed by which the SUT is raster imaged is much slower than the speed by which the p-i-n diodes can be turned "ON" and "OFF." Both signals are detected by a simple detector diode located at some prescribed distance along the probing waveguide and away from the aperture, as shown in Fig. 2(b). The loaded dipoles are positioned such as to modulate the dominated mode aperture field. Due to the reflection at the aperture, a standing wave is formed inside the waveguide. The utilized diode detector produces a dc voltage proportional to the power of the total probed signal in the waveguide. The detector dc voltage is measured using a typical digital voltmeter (DVM). Although using a standing-wave probing device makes the realization of the proposed probe simple, it is not the only implementation option. In fact, any coherent or noncoherent reflectometer-based detection system can be used in conjunction with this dual-modulated waveguide aperture probe. Similar to the differential probe proposed in [5], this method allows for 1-D standoff distance compensation. However, it is possible to obtain 2-D standoff compensation using the proposed method by synthesizing four aperture distributions. To this end, a different waveguide aperture shape such as a square aperture may be used [4].

III. Simulation Results

Extensive electromagnetic numerical simulations were carried out to validate the concept behind the proposed probe and to investigate various probe attributes, such as sensitivity and resolution as a function of its design parameters, i.e.,

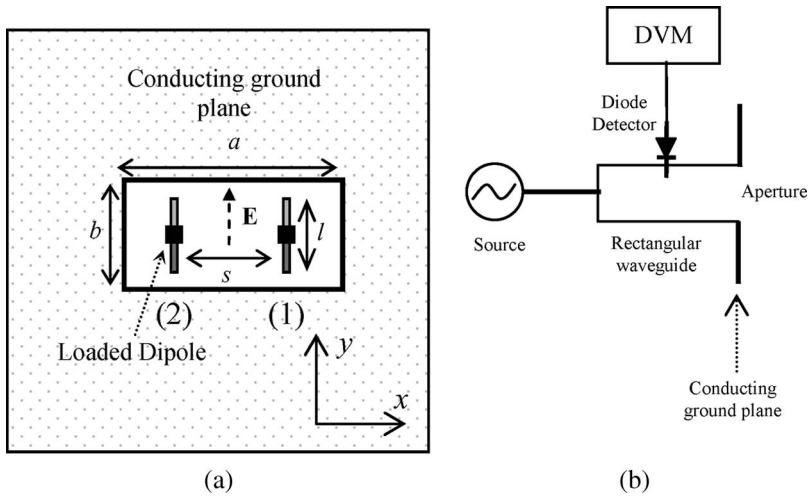

Fig. 2. (a) Schematic of the dual-loaded aperture with two loaded dipoles. (b) Standing-wave probing device incorporating the dual-loaded aperture probe.

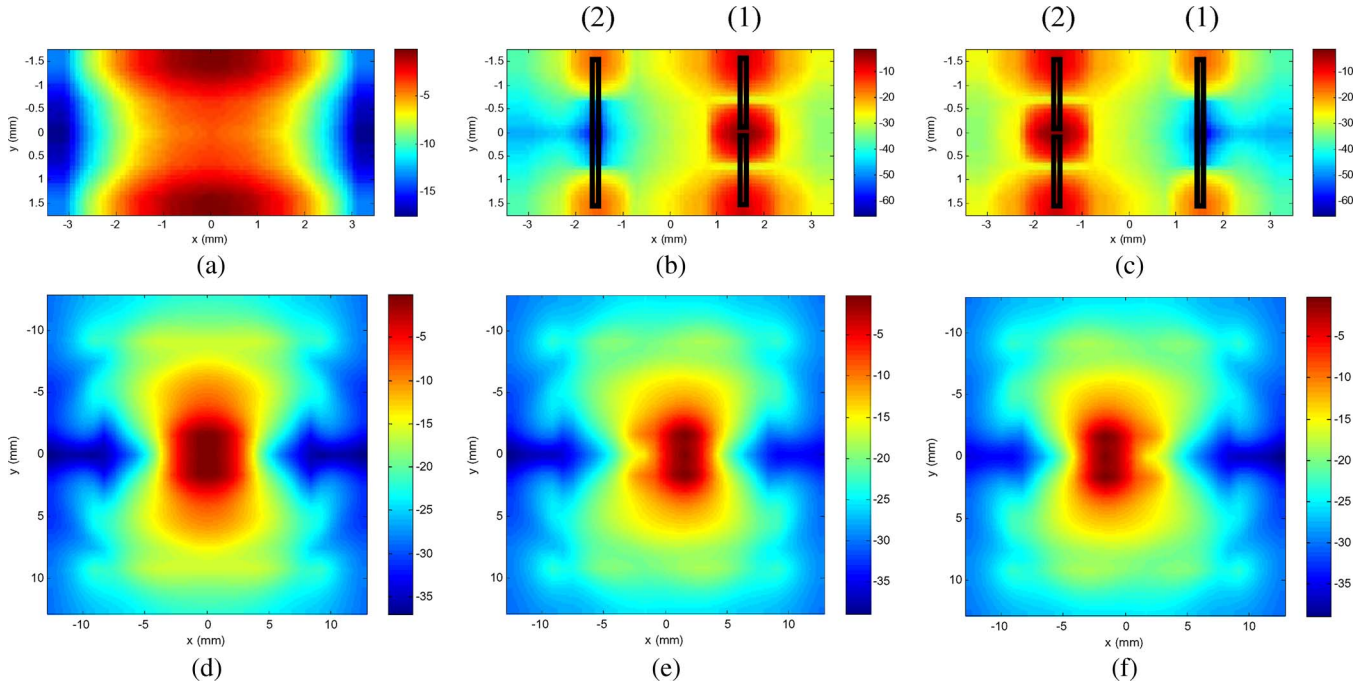

Fig. 3. Aperture normalized electric field distribution (in decibels) at 33.5 GHz for the (a) unloaded aperture, (b) dual-loaded aperture when dipole (1) is open-circuited, (c) dual-loaded aperture when dipole (2) is open-circuited, and (d)–(f) normalized electric field distribution 1 mm away from the apertures in (a)–(c), respectively.

the dipole interspacing s and the dipole length l. For this purpose, the CST Microwave Studio commercial simulation package was used [9]. A Ka-band (26.5–40 GHz) probe with a standard waveguide aperture ($a = 7.11$ mm; $b = 3.56$ mm) was considered for simulations. To validate the conceptual idea of synthesizing two mirror electric field distributions over a single aperture by using two identical loaded dipoles, the relative 2-D electric field distribution (magnitude) over the waveguide aperture was computed when the waveguide is radiating into free space at 33.5 GHz. Fig. 3(a) shows the normalized electric field distribution for the unloaded waveguide aperture (in decibels). Fig. 3(b) shows the aperture electric field distribution when it is dual loaded with two dipoles each of length $l = 3$ mm and separated by $s = a/2$ ($\sim$3.56 mm) while one of them [dipole (2)] is short-circuited and the other one [dipole (1)] is open-circuited. As shown in Fig. 3(b), the electric field distribution is skewed with its peak shifted toward the open-circuited dipole [dipole (1)]. This effect is reversed when dipole (1) is short-circuited while dipole (2) is open-circuited, as shown in Fig. 3(c). Fig. 3(d)–(f) shows the electric field distribution computed 1 mm away from the aperture over an area of $\sim$25 mm $\times$ 25 mm in the xy plane for the aforementioned loading conditions, respectively. By comparing Fig. 3(d) with 3(e) and (f), it is evident that the relative shift of the electric field pattern outside the aperture region follows the shift direction of the corresponding aperture fields. These results demonstrate the ability of synthesizing mirror near-field patterns using a single waveguide aperture and two reversed aperture loading conditions.

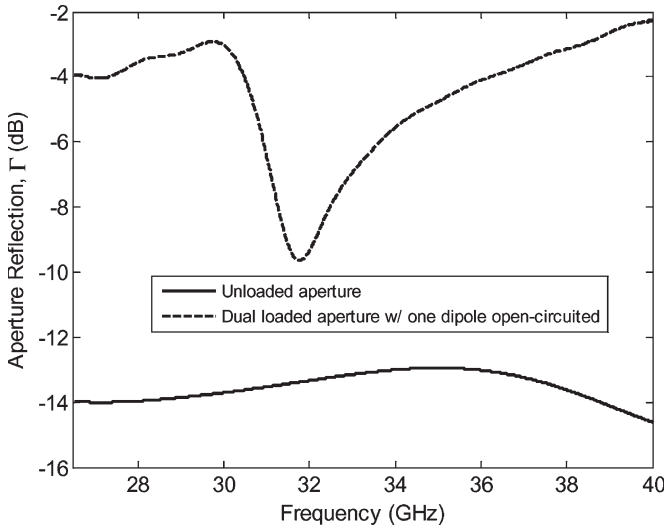

Fig. 4. Magnitude of the aperture reflection coefficient for unloaded and dual-loaded Ka-band waveguide apertures (one dipole is open-circuited, and the other is shorted).

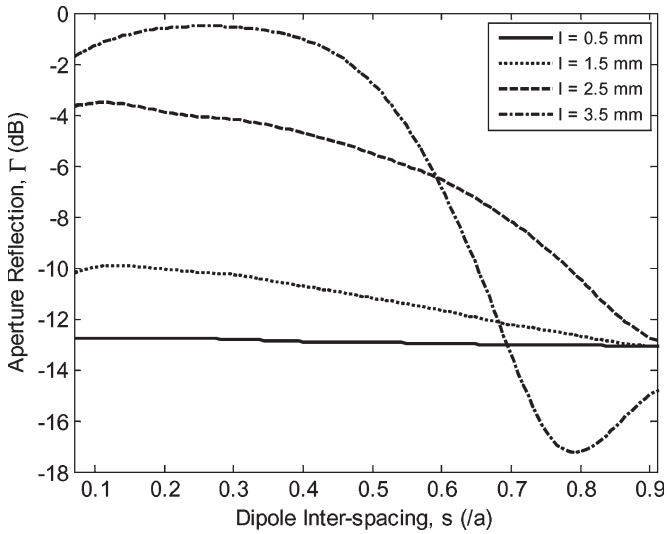

Fig. 5. Magnitude of the aperture reflection coefficient for a dual-loaded aperture as a function of dipole interspacings and lengths at 33.5 GHz (one dipole is open-circuited, and the other is shorted).

In general, loading the waveguide aperture with two dipoles increases the aperture reflection, as compared with the unloaded aperture. To quantify this effect, the magnitude of the aperture reflection coefficient (Ka-band) when one of the dipoles was open-circuited and the other one was short-circuited is shown in Fig. 4 for a dipole length of $l = 3$ mm and a dipole interspacing of $s = a/2$. Fig. 4 reveals that the dual-loaded aperture structure behaves like a resonant circuit with a very low Q-factor around the middle of the band due to the placement of the dipoles. To maximize the probe sensitivity, it is desirable to operate at frequencies where the inherent aperture reflection is relatively small, e.g., in the range from 30 to 34 GHz for this case. Although not shown here, the aperture complex reflection coefficient (phase and magnitude) remains the same when the loading condition is reversed. Furthermore, the aperture reflection coefficient depends on both the length of the dipoles and their interspacing. Such dependence is illustrated in Fig. 5,

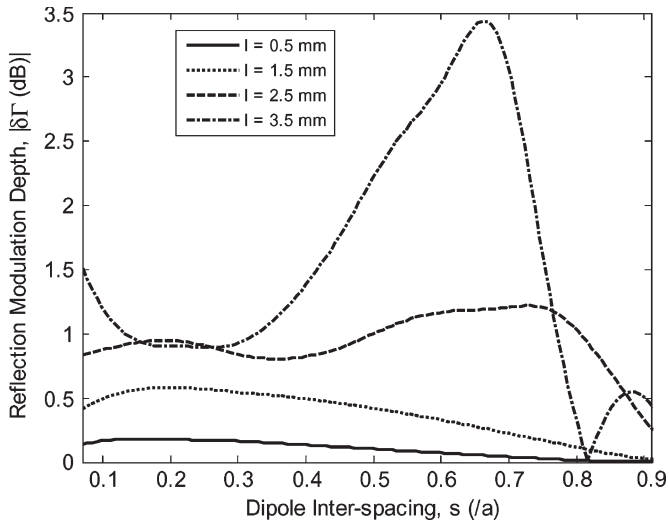

Fig. 6. Reflection modulation depth for a dual-loaded aperture as a function of dipole interspacings and lengths at 33.5 GHz.

where the magnitude of the reflection coefficient is plotted as a function of the dipole interspacing (normalized to the aperture broad dimension a) for different dipole lengths when one of the dipoles is open-circuited and the other one is short-circuited at a frequency of 33.5 GHz. As shown in Fig. 5, the aperture reflection coefficient is relatively large for longer dipoles and smaller dipole interspacings. This is expected since with a small interspacing, the dipoles are located around the center of the aperture and consequently cause maximum field blockage and, hence, reflection. On the other hand, using very short dipoles results in a smaller reflection coefficient with a weak dependence on the dipole interspacing. Although utilizing very short dipoles seems attractive for this type of aperture design, using such small dipoles does not cause a sufficient change in the aperture reflection coefficient, and the resulting signal might not be detected, as will be explained next.

As previously mentioned, the design of the proposed probe is based on modulating the dual-loaded aperture to synthesize the required field distributions. At any given scan point, the modulation cycle is a result of applying two consecutive loading conditions. The first loading condition is when one of the dipoles is open-circuited while the other one is short-circuited, and the second loading condition is when both dipoles are short-circuited. The relative change in the measured signal between these two conditions defines the so-called *modulation depth*. The sensitivity of the proposed method is directly proportional to the modulation depth. Hence, it is desired to design the probe with the maximum possible modulation depth. Fig. 6 shows the reflection modulation depth as a function of the dipole interspacing for different dipole lengths at 33.5 GHz. In line with the preceding definition, the modulation depth curves shown in Fig. 6 were computed as the absolute difference between the aperture reflections (in decibels) resulting after applying the aforementioned consecutive loading conditions while the aperture is radiating into free space. It is evident from Fig. 6 that the maximum modulation depth is obtained for longer dipoles and interspacing around $0.65a$. As shown in Fig. 6, using very short dipoles results in a very small modulation depth (< 0.25 dB),

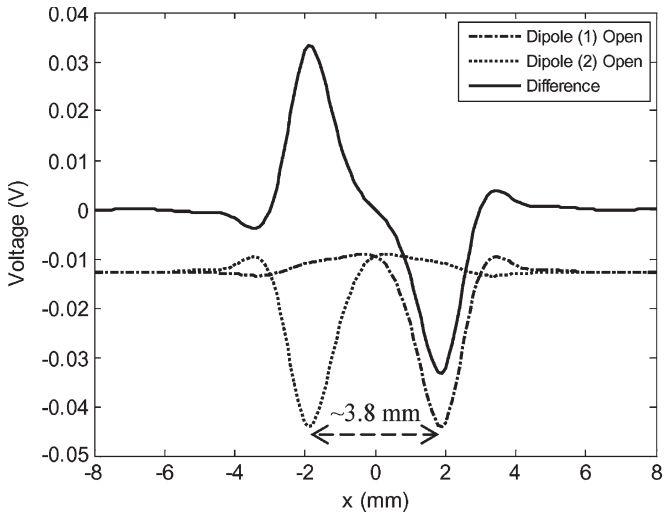

Fig. 7. Simulated 1-D scan of a thin metallic wire at 33.5 GHz.

and consequently, the change in the signal due to switching between the loading conditions might be hard to detect due to the limited sensitivity of the typical diode detectors.

In an imaging process, the target interacts with both of the synthesized near-field patterns/distributions. This interaction results in two aperture reflections at any scan point. To simulate the actual probe voltage response, each of the computed aperture reflections was converted to a standing-wave voltage via the relation $V_i = C|1 + \Gamma_i e^{-2j\beta L}|^2$, where V_i and Γ_i $(i = 1, 2)$ are the standing-wave voltage and aperture complex reflection coefficient, respectively, when the ith near-field pattern is switched "ON" (i.e., when the appropriate dipole is open-circuited), β is the propagation constant, L is the distance between the detector location and the aperture plane, and C is a constant proportional to the detector diode power–voltage conversion coefficient and the source power. The parameters L and C depend on the design of the standing-wave probing device, and they do not influence the basic operation of the proposed probe. Typical values for L and C (e.g., 30 mm and -0.035 V, respectively) were used in the simulations to predict the probe voltage response from the computed complex reflection coefficients.

To illustrate the differential probe response in imaging scenarios, a 1-D scan of a very thin 20-mm-long metallic wire aligned with the y-axis and placed at a distance of 1 mm from the aperture was subsequently simulated. The diameter of the wire was set to 0.1 mm, and its length was centered on the center of the aperture. The dipole lengths were 3 mm with a dipole interspacing of $s = 3.56$ mm. Fig. 7 shows the probe voltage response when dipole (1) was open-circuited while dipole (2) was short-circuited, the reverse condition, and the voltage difference between these two conditions, i.e., the differential response. The results shown in Fig. 7 were produced at 33.5 GHz. It is observed that when dipole (1) is open-circuited, the field pattern shown in Fig. 3(e) interacts with the target, and accordingly, the target indication is shown to be shifted toward the location of dipole (1). The same applies for the case when dipole (2) is open-circuited, where the field pattern shown in Fig. 3(f) interacts with the target. Due to subtracting both responses, the differential response shows two indications for the target, i.e., high (positive) and low (negative). The distance between the highest and lowest points of the target indications is approximately equal to the dipole interspacing, as shown in Fig. 7. Similar to the results reported in [5], the proposed differential probe produces target indications with odd symmetry around the center of the aperture.

The probe *imaging resolution* is another critical attribute that was also investigated in-depth via simulations. The probe resolution is defined here as the minimum distance between two detectable targets for which the probe is capable of producing two distinct indications. Fig. 8 shows the simulated differential probe voltage response when the probe was used to scan two thin wires separated by distances $t_s = 1$ mm [see Fig. 8(a)], 2 mm [see Fig. 8(b)], and 5 mm [see Fig. 8(c)]. The wires were of a diameter of 0.1 mm and a length of 20 mm, oriented along the y-axis while placed 1 mm away from the aperture. The aperture dipoles, each with a length of $l = 3$ mm, were separated by $s = 3.56$ mm, and the scan was produced at a frequency of 33.5 GHz as before. Again, it is observed that the probe response exhibits the typical differential odd symmetry. As shown in Fig. 8(a), the probe was not able to individually resolve the targets when they were 1 mm apart. In fact, the obtained response for $t_s = 1$ mm is similar in shape to the response when a single target was scanned with the proposed differential probe (see Fig. 7). The probe, however, started producing clear indications of the two targets when they were 2 mm apart, as depicted in Fig. 8(b). As the interspacing between the targets increased to 5 mm, the differential response produced two indications (high and low) for each target, as shown in Fig. 8(c).

Unlike the conventional open-ended waveguide probe near-field imaging resolution, which is solely limited by the aperture broad dimension a, the proposed differential probe resolution is a function of the loaded dipole interspacing. In general, finer resolution can be obtained with a small dipole interspacing. For illustration purposes, the proposed probe was used to scan the previously described targets with $t_s = 2$ mm using a dual-loaded aperture with dipole interspacings $s = a/2$ and $s = 3a/4$. Fig. 9 shows the differential probe voltage response for these two dipole interspacings. As shown in Fig. 9, while the targets were not resolved when the dipole interspacing was $s = 3a/4$, the probe with $s = a/2$ was capable of resolving both targets. It is important to note that the probe resolution, as opposed to its sensitivity, is not a function of the dipole length. Finally, it is also important to observe that the obtained resolution using the proposed probe, as shown here, is in fact finer than the resolution offered by the conventional open-ended waveguide probe. In the near field, the spatial resolution obtained using open-ended waveguide imaging probes is lower bounded by half the probe aperture broad size, i.e., $a/2$ ($\sim$3.56 mm) [10]. On the other hand, the proposed probe yielded a resolution of around 2 mm, as indicated in the simulation results.

IV. Measurement Results and Discussion

As shown in Fig. 2(a), the dipoles are aligned in parallel with the aperture dominant-mode electric field polarization and used here as parasitic elements to synthesize the desired field

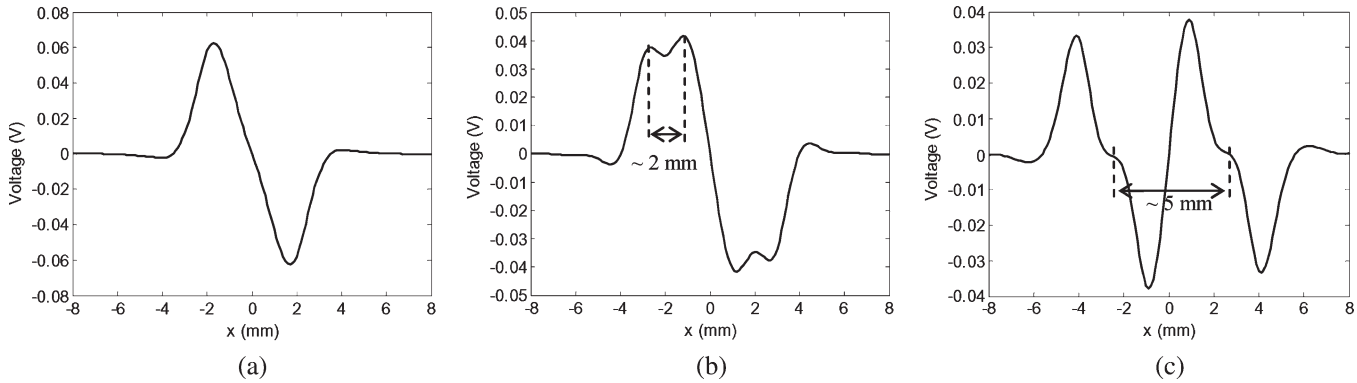

Fig. 8. Simulated differential probe voltage response when the probe was used to scan two linear targets as a function of the target interspacing at 33.5 GHz ($s = a/2$).

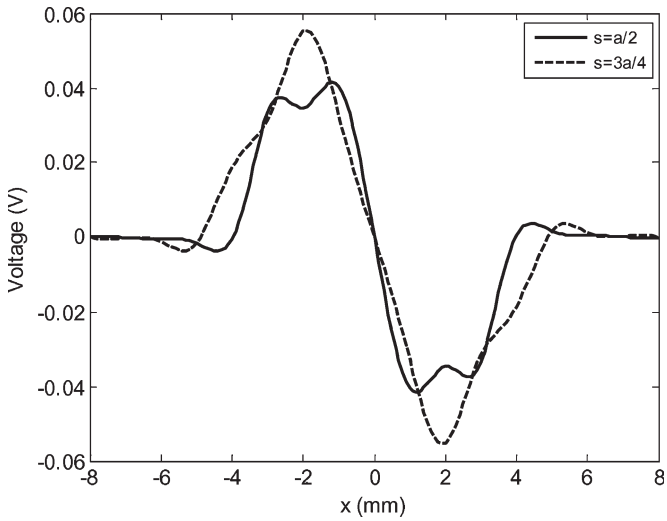

Fig. 9. Simulated differential probe voltage response with $s = a/2$ and $s = 3a/4$ when the probe was used to scan two linear targets spaced by 2 mm at 33.5 GHz.

distribution by electronically controlling the loads [11]. To this end, p-i-n diodes are used to load the dipoles in practice [7], [8]. The desired distribution can be switched "ON" and "OFF" by forward and reverse biasing the appropriate diode, respectively. Typically, microwave and millimeter-wave p-i-n diodes switch between forward and reverse states quite fast, e.g., on the order of nanoseconds, and thus, the delay due to the switching time does not lengthen the overall scan time. With the developed probe, at least one modulation cycle is needed at each scan location to switch between the patterns. When using fast-switching millimeter p-i-n diodes as the ones used here, the modulation cycle width can be on the order of hundreds of nanoseconds. The total scan time can be approximated as $T_{\text{total}} \approx N[t + t_m + t_a]$, where N is the total number of scan points, t is the time required to move the probe, t_m is the modulation cycle width, and t_a is the time required to acquire the data at each point. For typical scanning platforms and data acquisition cards, t and t_a are on the orders of a few milliseconds and hundreds of microseconds, respectively. Thus, the total scan time is in fact dominated by those two components and not by the diode switching time.

To experimentally demonstrate the efficacy of the proposed probe, a Ka-band prototype probe was manufactured and tested. A standard Ka-band rectangular waveguide aperture with printed dipoles was fabricated using a two-layer 0.508-mm-thick printed circuit board (PCB) with a Rogers-4350 substrate material ($\varepsilon_r = 3.48$ and a loss tangent of 0.004). The aperture was etched out on both sides of the PCB, and the ground planes were connected by small vias around the aperture. The substrate was sufficiently thin such that it does not significantly impact the aperture reflection. The dipoles, each of length 3 mm and width 0.25 mm, were printed on the top layer of the PCB and symmetrically placed about the center of the aperture with an interspacing distance of $s = 3a/4$ (5.3 mm). The dipoles were loaded by two identical flip-chip p-i-n diodes (0.7 mm $\times$ 0.38 mm) controlled by dc bias lines (0.25 mm wide). The bias lines were routed through the top ground plane. In the aperture region, the bias lines were routed such that they were orthogonal to the dominant-mode electric field polarization, and hence, their perturbing effect was minimized. The used p-i-n diodes needed 1.45 V to switch between the reverse and the forward states. When reverse biased, the diode represents a capacitive load of 25 fF, and in the forward state, it is equivalent to a 5-Ω resistive load. The used p-i-n diodes switch in less than 5 ns, and hence, the modulation frequency can be as high as 200 MHz. Additionally, 5-pF small surface-mount (SMT) capacitors (0.5 mm $\times$ 0.25 mm) were used to realize an RF return path to ground (short-circuit) for any signal that might couple into the dc bias lines, thus preventing any spurious radiation or resonances that could result from such coupling. Fig. 10 shows a magnified picture for the top layer and the modulated aperture components. The aperture was fed from the bottom layer side by a Ka-band rectangular waveguide with a standing-wave probing device, as shown in Fig. 2(b).

The symmetry in the probe response as the diodes are switched/modulated is critical for proper probe operation. The probe should produce identical responses for the reversed aperture loading conditions when it radiates into a medium with no lateral spatial variations. The response symmetry was tested first by measuring the aperture complex reflection coefficient using a vector network analyzer and then by modulating both diodes while the aperture is radiating into free space. Fig. 11 shows the measured complex reflection coefficient when diode (1) was "ON" while diode (2) was "OFF," and *vice versa*. As depicted in Fig. 11, the reflection measurements for both states are very close. The discrepancies between the measurements for

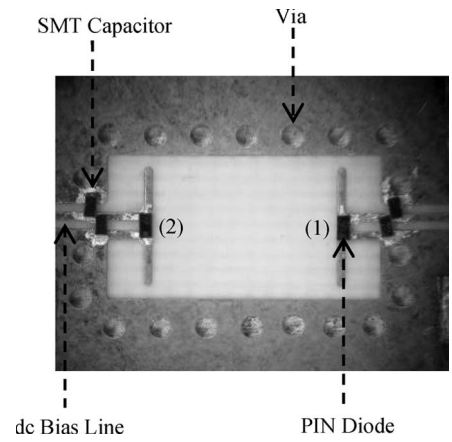

Fig. 10. Magnified picture of the manufactured prototype Ka-band dual-loaded aperture.

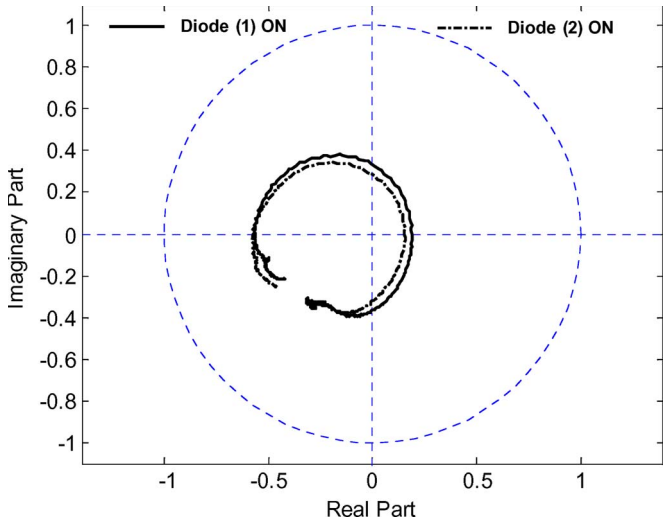

Fig. 11. Dual-loaded aperture complex reflection coefficient over the Ka-band for both diode states.

the two modulation states are mainly attributed to the physical differences of the diodes and their biasing structures. Such discrepancy is marginal and will not impact the overall probe symmetry when the standing-wave measurement device is used, as will be shown next. Fig. 12 shows the measured standing-wave voltage over five modulation cycles for both diodes while the probe was operating at 33.5 GHz. As shown in Fig. 12, the response in the "ON" and "OFF" states for both diodes is almost identical. This, in turn, validates the symmetry exhibited in the probe design.

To examine the response of the proposed probe to standoff distance variations, a conducting plate was flushed against the aperture of the waveguide and subsequently gradually moved away in the direction normal to the aperture, as schematically depicted in Fig. 13(a). Fig. 13(b) shows the measured standing-wave voltage as a function of the standoff distance normalized to the free-space wavelength λ at 33.5 GHz. The three traces in Fig. 13(b) correspond to the cases when the first diode was "ON" while the second diode was "OFF," when the first diode was "OFF" while the second one was "ON," as well as the voltage difference between these two states. The response due

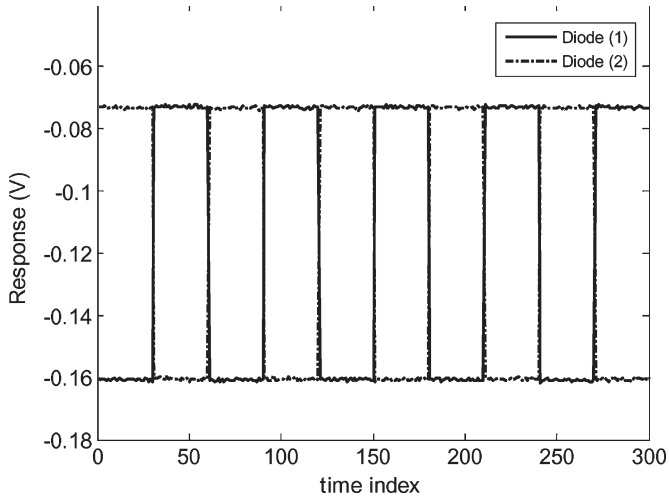

Fig. 12. Modulated response for both diodes at 33.5 GHz.

to the first two cases is rather typical for this type of measurements, i.e., standing-wave voltage measurements, using a single-aperture probe [1]. Furthermore, these two cases resulted in almost identical voltage responses, as expected. Therefore, the voltage difference between these states, i.e., the differential response, shows minimal variations with the standoff distance, e.g., around 10 mV peak to peak. It is also apparent that the compensation range extends beyond one wavelength. The differential response exhibits small peaks at about every $\lambda/2$, as depicted in Fig. 13(b). Because the dipoles and their loads are not perfectly identical, the phases of the reflection coefficients for both loading conditions are slightly shifted with respect to each other. Due to this inherent phase shift, the standing wave corresponding to each loading condition will slightly be shifted with respect to the other loading condition. Hence, the difference between the responses of both loading conditions will not be identically zero. This effect is prominently manifested as peaks shown about every $\lambda/2$ in the differential response since the phase of the reflected signal jumps around $\pm 180^{\circ}$ at these points. Similar behavior was also observed for the coherent differential probe proposed in [5].

Before using the proposed probe for imaging localized targets, it is important that the prototype probe response is well understood. For this purpose, the probe was used to produce linear scans of a thin metallic wire at 33.5 GHz. Fig. 14(a) shows a schematic for the cross section of the target–probe experimental setup. The wire was much longer than the aperture narrow-side b. The diameter of the wire was 0.5 mm, and it was located at a fixed standoff distance of 1 mm from the aperture. Fig. 14(b) shows the obtained linear scans. It is observed that the scans obtained with both modulation states (diode (1) was "ON" while diode (2) was "OFF," and diode (1) was "OFF" while diode (2) was "ON") are symmetric around the aperture center (the aperture broad-side center coincides with $x = 30$ mm). Each of these line scans is slightly shifted from the aperture center. This observation experimentally confirms the applicability of the approach to synthesize two symmetric field distributions by using a single aperture. In addition to the main lobe, the linear scans with both states show small sidelobes near the position of the open-circuited dipole. In near-field imaging,

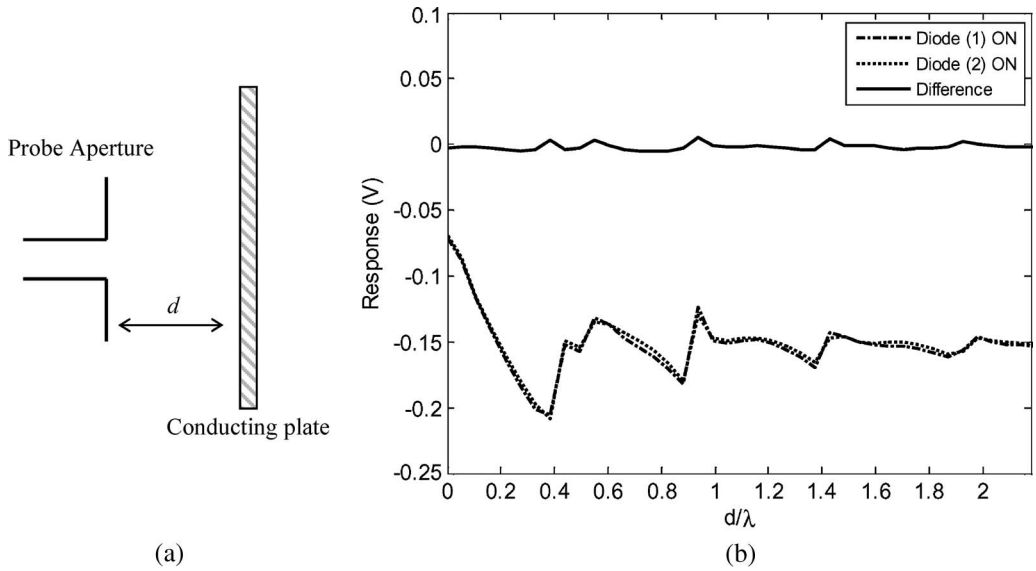

Fig. 13. (a) Standoff distance variation experimental setup. (b) Measured standing-wave voltage as a function of the normalized standoff distance.

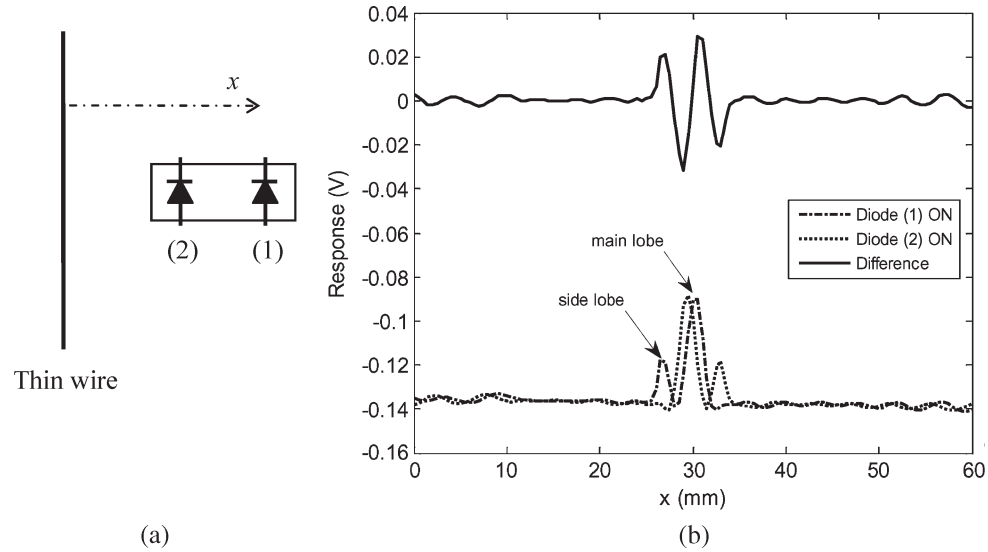

Fig. 14. (a) Schematic for the cross section of the target–probe experimental setup. (b) Obtained 1-D scan of a thin metallic wire at 33.5 GHz.

these sidelobes are expected to interact with the imaged target as well. The differential linear scan shown in Fig. 14(b) was obtained as the difference between the linear scans for both modulation states. As such, it shows odd symmetry around the aperture center. That is, the target indication is two sided, i.e., high (positive) and low (negative), as it was observed in the simulation results. Consequently, in 2-D images, a target will be manifested by two colors, e.g., black and white in gray-scale images, as it will be shown later in this paper. It is also interesting to visualize the probe response to the 2-D target with width comparable to the dipole interspacing. Fig. 15 shows the linear scan obtained for a thin copper strip of width $\sim$6.25 mm placed 1 mm away from the aperture with its length along the y-axis. Again, the strip was much longer than the waveguide narrow dimension. Due to the interaction of both strip edges with the probe, the target indication is not as simple as in the thin-wire case. Each strip edge results in two mirror indications, as shown by the differential response in Fig. 15.

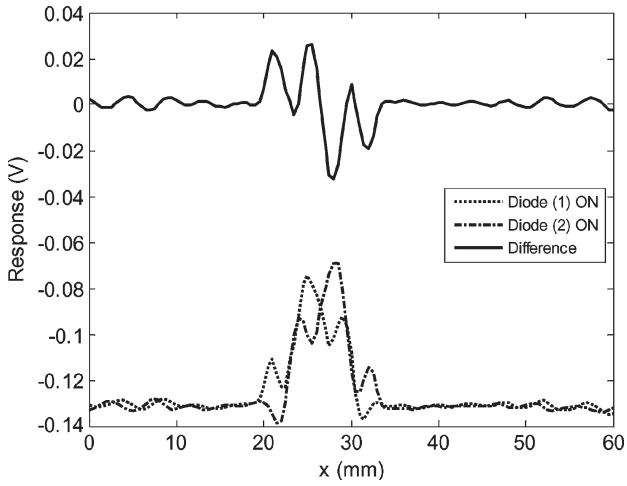

Fig. 15. One-dimensional scan of a thin copper strip of width 6.25 mm obtained at 33.5 GHz.

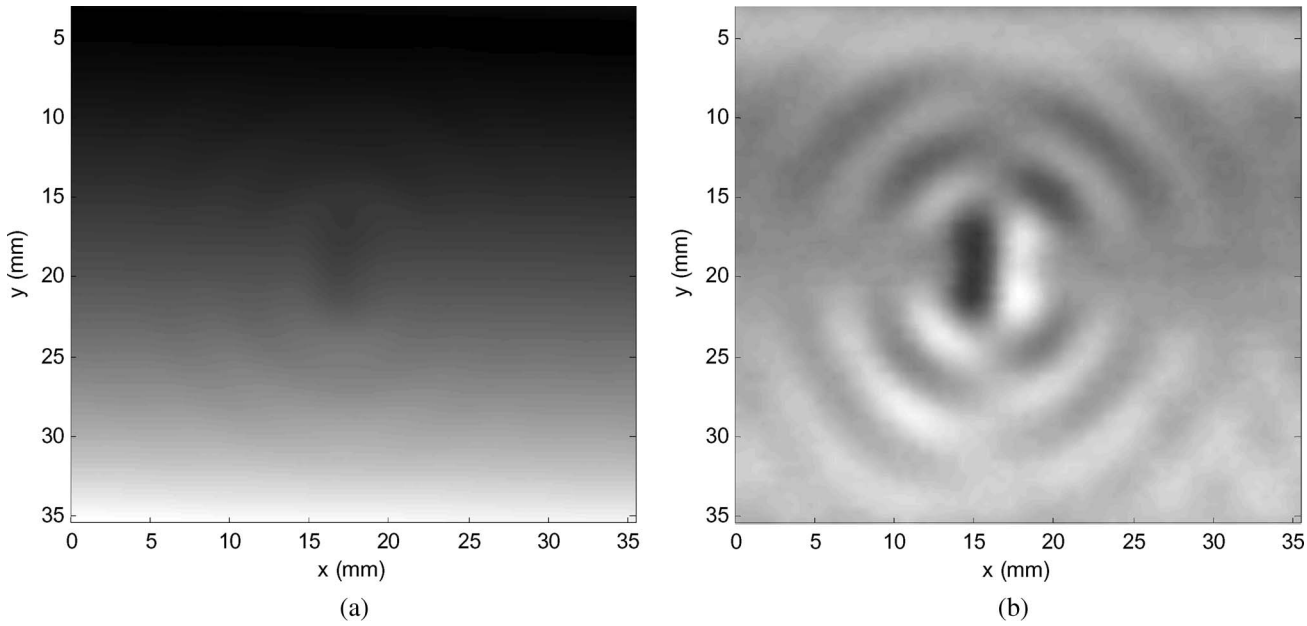

Fig. 16. Images of a small hole in a slanted conducting plate as obtained using the (a) conventional standing-wave probe and (b) proposed differential probe.

TABLE I
COMPARISON BETWEEN VARIOUS DIFFERENTIAL PROBES AND COMPENSATION METHODS

Probe	Advantages	Disadvantages	Category
In-Contact Compensator [3]	Simple 2D compensation	needs calibration & contact, <λ\4 compensation range	Non- coherent
Dual polarized probe [4]	Simple	needs calibration, applicable to special structures only, <λ\4 compensation range	Non-coherent
Dual-loaded modulated aperture probe (proposed)	Simple, >λ compensation range, easily optimized, high resolution,	Switching delay	Non-coherent
Dual-aperture differential probe [5]	>λ compensation range	Relatively complex	Coherent

To highlight the utility of the proposed probe for near-field imaging, it was used to image a small cylindrical hole (∼2 mm in diameter and ∼2 mm in depth) in a metallic plate while the plate was slanted with a large angle (to simulate a severe standoff distance variation). For comparison purposes, the same hole was imaged using a conventional single-aperture standing-wave probe [1]. Fig. 16(a) and (b) shows the obtained images at 33.5 GHz using the conventional probe and the dual-loaded differential probe, respectively. While the indication of the hole is faint and almost masked by the standoff distance variations in the image produced using the conventional probe, it is clearly visible in the differential probe image. The latter image clearly shows the utility of this approach for near-field microwave and millimeter-wave imaging. The odd symmetry observed in the linear scans is also shown in the image obtained by the differential probe. Therein, the indication of the hole is both the brightest white and darkest black regions in the center of the image. The odd symmetry also applies for the probe aperture sidelobes, which interact with the hole as well. The sidelobe effect is shown in Fig. 16(b) as concentric rings. The odd symmetry response attributes of the proposed differential probe is in fact similar to that of the coherent differential probes [5].

Finally, to clearly define the scope of application, Table I summarizes the major advantages and disadvantages of the proposed probe and compares between the various developed differential probes and compensation methods.

V. CONCLUSION

A novel microwave and millimeter-wave differential probe has been designed based on dual loading and modulating a single waveguide aperture. The proposed probe was shown to combine the attractive features of the coherent and noncoherent probes, namely, versatility and simplicity, in a compact design. The idea behind the proposed probe, i.e., synthesizing two mirror electric field distributions through dual-aperture loading, was verified via simulations and experiments. Extensive numerical simulations were performed to study the design parameters that impact the probe sensitivity and resolution.

A Ka-band prototype probe was experimentally designed and tested. The symmetry of the probe design was confirmed, and the probe response to standoff distance variations was investigated as well. It was shown that the proposed probe efficiently reduces the standoff distance variations based on simple noncoherent detection. Scanning the 1-D target verified the basic principle of synthesizing two symmetric aperture field distributions using a single waveguide aperture dual modulated by loaded dipoles. Furthermore, the linear scans provided insight into the expected response when the probe was subsequently used for 2-D scans. The image obtained for a localized target in severe standoff distance variations setup demonstrated the potential of the proposed probe for near-field microwave and millimeter-wave imaging. The various features in the obtained image were in line with observations drawn from the simulation results and the experimental linear scans. With the proposed approach, 2-D standoff distance compensation using a rectangular aperture with two diodes might be feasible by processing two additional modulation states: both diodes OFF/ON. This scheme, along with using a square waveguide aperture, will be the subject of future investigation.

ACKNOWLEDGMENT

The authors would like to thank Dr. D. Pommerenke and Dr. J. Drewniak of the EMC Laboratory, Missouri University of Science and Technology, for facilitating some of the measurements presented in this paper by providing us with the use of their laboratory equipment.

REFERENCES

[1] R. Zoughi, *Microwave Non-Destructive Testing and Evaluation*. Dordrecht, The Netherlands: Kluwer, 2000.

[2] C. A. Balanis, *Advanced Engineering Electromagnetic*. New York: Wiley, 1989.

[3] N. Qaddoumi, T. Bigelow, R. Zoughi, L. Brown, and M. Novack, "Reduction of sensitivity to surface roughness and slight standoff distance variations in microwave testing of thick composite structures," *Mater. Eval.*, vol. 60, no. 2, pp. 165–170, Feb. 2002.

[4] S. Kharkovsky, A. C. Ryley, V. Stephen, and R. Zoughi, "Dual-polarized near-field microwave reflectometer for noninvasive inspection of carbon fiber reinforced polymer (CFRP) strengthened structures," *IEEE Trans. Instrum. Meas.*, vol. 57, no. 1, pp. 168–175, Jan. 2008.

[5] M. T. Ghasr, B. Carroll, S. Kharkovsky, R. Austin, and R. Zoughi, "Millimeter-wave differential probe for nondestructive detection of corrosion precursor pitting," *IEEE Trans. Instrum. Meas.*, vol. 55, no. 5, pp. 1620–1627, Oct. 2006.

[6] M. A. Abou-Khousa and R. Zoughi, "Novel near-field microwave and millimeter wave differential probe using a dual-modulated single aperture," in *Proc. IEEE IMTC*, Victoria, BC, Canada, May 2008, pp. 442–445.

[7] J. H. Richmond, "A modulated scattering technique for measurement of field distributions," *IEEE Trans. Microw. Theory Tech.*, vol. MTT-3, no. 4, pp. 13–15, Jul. 1955.

[8] R. Janaswamy and S.-W. Lee, "Scattering from dipoles loaded with diodes," *IEEE Trans. Antennas Propag.*, vol. 36, no. 11, pp. 1649–1651, Nov. 1988.

[9] CST—Computer Simulation Technology. [Online]. Available: http://www.cst.com/Content/Products/MWS/Overview.aspx

[10] N. N. Qaddoumi, M. Abou-Khousa, and W. M. Saleh, "Near-field microwave imaging utilizing tapered rectangular waveguides," *IEEE Trans. Instrum. Meas.*, vol. 55, no. 5, pp. 1752–1756, Oct. 2006.

[11] R. Harrington and J. Mautz, "Straight wires with arbitrary excitation and loading," *IEEE Trans. Antennas Propag.*, vol. AP-15, no. 4, pp. 502–515, Jul. 1967.

Mohamed A. Abou-Khousa (S'01) was born in Al-Ain, United Arab Emirates, in 1980. He received the B.S.E.E. degree (*magna cum laude*) from the American University of Sharjah, Sharjah, United Arab Emirates, in 2003 and the M.S.E.E. degree from Concordia University, Montreal, QC, Canada, in 2004. He is currently working toward the Ph.D. degree in electrical engineering with the Missouri University of Science and Technology (Missouri S&T; formerly University of Missouri-Rolla), Rolla.

Since January 2005, he has been with the Applied Microwave Nondestructive Testing Laboratory (AMNTL), Missouri S&T, as a Graduate Research Assistant. His current research interests include millimeter-wave and microwave instrumentation, numerical electromagnetic analysis, reconfigurable antennas, and wideband wireless communication systems.

Mr. Abou-Khousa frequently serves as a reviewer for various IEEE technical publications. He was a recipient of the First Prize Award at the IEEE IAS 2003 Myron Zucker Student Design Contest.

Sergey Kharkovsky (M'01–SM'03) received the M.S. degree in electronics engineering from Kharkov National University of Radioelectronics, Kharkov, Ukraine, in 1975, the Ph.D. degree in radiophysics from Kharkov State University in 1985, and the D.Sc. degree in radiophysics from the National Academy of Sciences of Ukraine, Kharkov, in 1994, respectively.

He is currently a Research Associate Professor with the Department of Electrical and Computer Engineering, Missouri University of Science and Technology (Missouri S&T; formerly University of Missouri-Rolla), Rolla. Prior to joining Missouri S&T in March 2003, he was a Member of Research Staff with the Institute of Radio-Physics and Electronics (IRE), National Academy of Sciences of Ukraine, from 1975 to 1998, and a Professor with the Department of Electrical and Electronics Engineering, Cukurova University, Adana, Turkey, from December 1998 to February 2003. He was a Visiting Associate Professor with the Department of Electrical and Computer Engineering, Missouri S&T, from March 2003 to February 2006. His research area at IRE was the investigation and development of new millimeter-wave techniques, including dielectric resonators with whispering gallery modes and solid-state oscillators and their application for material characterization. His current research interest is nondestructive evaluation of composite structures using microwaves and millimeter waves.

Reza Zoughi (S'85–M'86–SM'93–F'06) received the B.S., M.S., and Ph.D. degrees from the University of Kansas, Lawrence, all in electrical engineering (radar remote sensing, radar systems, and microwaves).

From 1981 until 1987, he was with the Radar Systems and Remote Sensing Laboratory (RSL), University of Kansas. He is currently the Schlumberger Endowed Professor of Electrical and Computer Engineering with Missouri University of Science and Technology (Missouri S&T; formerly University of Missouri-Rolla), Rolla. Prior to joining Missouri S&T in January 2001, in 1987, he joined the Department of Electrical and Computer Engineering, Colorado State University (CSU), Fort Collins, where he was a Professor. He held the position of the Business Challenge Endowed Professor of Electrical and Computer Engineering from 1995 to 1997 while at CSU. He is the author of a textbook entitled *Microwave Nondestructive Testing and Evaluation Principles* (Kluwer, 2000) and the coauthor (with A. Bahr and N. Qaddoumi) of a chapter on microwave techniques in an undergraduate introductory textbook entitled *Nondestructive Evaluation: Theory, Techniques, and Applications* (edited by P. J. Shull; Marcel Dekker, 2002). He is the coauthor of more than 95 journal papers, 229 conference proceedings and presentations, and 81 technical reports. He is the holder of eight patents, all in the field of microwave nondestructive testing and evaluation.

Dr. Zoughi is a Fellow of the American Society for Nondestructive Testing (ASNT). He is the Editor-in-Chief of the IEEE TRANSACTIONS ON INSTRUMENTATION AND MEASUREMENT. He was the recipient of numerous teaching awards both at CSU and Missouri S&T.